Suppression of VEGF secretion and changes in glioblastoma multiforme microenvironment by inhibition of Integrin-linked kinase (ILK)

Lincoln A. Edwards,[1,5] Janet Woo,[1,5] Lynsey A. Huxham,[2] Maite Verreault,[1,5] Wieslawa H. Dragowska,[1] Gigi Chiu,[9] Ashish Rajput,[5] Alastair H. Kyle,[2] Jessica Kalra,[1,5] Donald Yapp,[1,7] Hong Yan,[1] Andrew I. Minchinton,[2,5] David Huntsman,[5] Tim Daynard,[8] Dawn N. Waterhouse,[1,7] B. Thiessen,[3,5] Shoukat Dedhar,[4,6] and Marcel B. Bally[1,3,5,7]

Departments of [1]Advanced Therapeutics, [2]Medical Biophysics, [3]Medical Oncology, and [4]Cancer Genetics, BC Cancer Agency; Departments of [5]Pathology and Laboratory Medicine and [6]Biochemistry and Molecular Biology and [7]Faculty of Pharmaceutical Sciences, University of British Columbia; [8]Department of Medicinal Chemistry, QLT, Inc., Vancouver, British Columbia, Canada; and [9]Department of Pharmacy, National University of Singapore, Republic of Singapore

Abstract

Integrin-linked kinase (ILK) was assesed as a therapeutic target in glioblastoma xenograft models through multiple endpoints including treatment related changes in the tumor microenvironment. Glioblastoma cell lines were tested *in vitro* for sensitivity toward the small-molecule inhibitors QLT0254 and QLT0267. Cell viability, cell cycle, and apoptosis were evaluated using MTT assay, flow cytometry, caspase activation, and DAPI staining. Western blotting and ELISA were used for protein analysis (ILK, PKB/Akt, VEGF, and HIF-1α). *In vivo* assessment of growth rate, cell proliferation, BrdUrd, blood vessel mass (CD31 labeling), vessel perfusion (Hoechst 33342), and hypoxia (EF-5) was done using U87MG glioblastoma xenografts in RAG2-M mice treated orally with QLT0267 (200 mg/kg q.d.). ILK inhibition *in vitro* with QLT0254 and QLT0267 resulted in decreased levels of phospho-PKB/Akt (Ser^{473}), secreted VEGF, G_2-M block, and apoptosis induction. Mice treated with QLT0267 exhibited significant delays in tumor growth (treated 213 mm^3 versus control 549 mm^3). *In situ* analysis of U87MG tumor cell proliferation from QLT0267-treated mice was significantly lower relative to untreated mice. Importantly, VEGF and HIF-1α expression decreased in QLT0267-treated tumors as did the percentage of blood vessel mass and numbers of Hoechst 33342 perfused tumor vessels compared with control tumors (35% versus 83%). ILK inhibition with novel small-molecule inhibitors leads to treatment-associated delays in tumor growth, decreased tumor angiogenesis, and functionality of tumor vasculature. The therapeutic effects of a selected ILK inhibitor (QLT0267) should be determined in the clinic in cancers that exhibit dysregulated ILK, such as PTEN-null glioblastomas. [Mol Cancer Ther 2008;7(1):59–70]

Introduction

Mutations in genes that encode selected receptor and intracellular kinases appear to be essential for cancer progression and metastasis (1). This knowledge has led to an evolution in anticancer drug design from nonspecific cytotoxic agents to highly selective ones, targeting molecules/proteins that are critical to cancer cell proliferation, survival, and/or metastasis (2). Targets that affect cell growth, proliferation, and apoptotic pathways are certainly important, but direct effects on the cancer cell often do not take into account how therapy influences the tumor microenvironment. The tumor microenvironment is represented by a collage of attributes encompassing variations in pH and blood vessel density as well as hypoxic and perfused regions (3). This, in addition to the mixed tumor cell and host cell populations that typify tumor heterogeneity, makes it easy to understand why cancer has been so difficult to treat effectively. For example, hypoxia-inducible factor-1α (HIF-1α) and vascular endothelial growth factor (VEGF) are key factors known to affect the tumor microenvironment and can be induced in response to hypoxia that in turn can lead to angiogenesis (4–6). Thus, an environmental crisis triggered by hypoxia can be mitigated by cellular pathways designed to promote angiogenesis. The tumor microenvironment allows the cancerous process to progress (promoting cell survival and adaptation), enhances the likelihood of metastatic spread (due to prostimulatory angiogenic factors), and creates conditions that foster development of resistance to traditional chemotherapeutic treatment (7–9).

Many approaches to targeting the tumor microenvironment have been pursued (10–12); however, here we propose an alternative approach that considers central

Received 5/11/07; revised 9/19/07; accepted 12/4/07.

Grant support: National Cancer Institute of Canada (including support from the Canadian Breast Cancer Research Alliance) and QLT, Inc. S. Dedhar was supported by grants from the National Cancer Institute of Canada with funds raised by the Canadian Cancer Society.

The costs of publication of this article were defrayed in part by the payment of page charges. This article must therefore be hereby marked *advertisement* in accordance with 18 U.S.C. Section 1734 solely to indicate this fact.

Requests for reprints: Dawn N. Waterhouse, Department of Advanced Therapeutics, BC Cancer Agency, Vancouver, British Columbia, Canada. E-mail: dwater@bccrc.ca

doi:10.1158/1535-7163.MCT-07-0329

pathways within cells that lead to multiple effects, including inhibition of tumor cell proliferation, induction of apoptosis, and inhibition of VEGF secretion. Integrin-linked kinase (ILK) exemplifies a target that is capable of producing these pleiotropic effects. ILK increases VEGF expression by stimulating HIF-1α via a phosphatidylinositol 3′-kinase (PI3K)–dependent activation of protein kinase B (PKB)/Akt (13). ILK has also been shown to promote cell growth (14) and cell cycle progression (15) and to inhibit apoptosis (16). Previously, we and others have shown the regulatory role of ILK in glioblastoma progression (17–20). We show that targeting ILK with small-molecule QLT0267 resulted in decreased VEGF and HIF-1α expression, effects that were associated with decreased hypoxia, decreases in tumor vascular mass, and decreases in functional vasculature.

Materials and Methods

Cell Culture and Reagents

Three human glioblastoma cancer cell lines were used in this study: the PTEN-positive SF-188 and the PTEN-negative U87MG and U251MG. Cells were cultured in DMEM containing 10% fetal bovine serum with 1% L-glutamine and 1% penicillin/streptomycin at 37°C in a humidified atmosphere containing 5% CO_2. For all experiments, cells were used in exponential growth phase.

Retroviral constructs with an inducible PTEN promoter (U87.23) were generously provided by Dr. Michael Wigler and were maintained with hygromycin selection at 50 μg/mL. Muristerone A (Invitrogen) was reconstituted in 100% ethanol before adding to cells for induction of PTEN. Cells were harvested 24 to 48 h following induction.

ILK inhibitors QLT0254 and QLT0267 were provided by QLT. Both inhibitors have been shown to be selective relative to other kinases (21–23) in cell-free recombinant kinase assays. QLT0267 has also been tested for selectivity versus PI3Ks in a cell-free recombinant kinase assay at 2 μmol/L and was found to inhibit PI3Kβ activity by 9%, PI3Kγ by 23%, and PI3Kδ by 15%. The IC_{50} for inhibition of ILK by QLT0267 was ~26 nmol/L and the IC_{50} for QLT0254 was 300 nmol/L in a cell-free assay (QLT; data on file). These are low molecular weight (<500) compounds that are administered in an oral dosage form. The parent structure of the pharmacophor used to prepare QLT0254 and QLT0267 is provided in Fig. 1A. ILK antisense designated here as "ILKAS" and transfection procedures have been previously described (17).

Cytotoxicity Assay

Growth inhibition of U87MG, U251MG, and SF-188 cells following exposure to ILK inhibitors was determined by the colorimetric 3-(4,5-dimethylthiazol-2-yl)-2,5-diphenyl tetrazolium bromide MTT assay. In brief, cells were plated at 10,000 per well in 96-well plates and allowed to adhere overnight before exposure to the ILK inhibitor QLT0254 or QLT0267 and then incubated for 24 or 48 h at 37°C. MTT was added to cells, and after 3-h incubation at 37°C, the purple formazan precipitate was solubilized in DMSO. Absorbance (562 nm) was determined in a microtiter plate reader (Dynex Technologies). The percentage of growth inhibition was calculated as an absorbance ratio of wells containing treated cells to untreated controls × 100%. All assays were done in triplicate. IC_{50}s for QLT0254 or QLT0267 were analyzed using the CalcuSyn software program (Biosoft; ref. 24).

Cell Cycle Analysis

Cells were cultured with or without drug treatment for 24 h and subsequently analyzed. Controls included untreated cells or cells treated with the vehicle control PTE cells [PEG_{300}/ethanol/Tween 80/citrate (63:29:7.8:0.2, w/v/w/w)]. Cells were harvested, fixed with cold 70% ethanol, and stored overnight at −20°C followed by staining with propidium iodide staining buffer (1 mg/mL RNase A, 0.1% Triton X-100, 50 μg/mL propidium iodide in PBS).

Stained samples were analyzed by flow cytometry with a FACSCalibur (Becton Dickinson) or with WinMDI 2.9 Freeware to determine cell cycle distribution. The percentage of cells in each cell cycle phase was calculated relative to total cells in G_1-G_0, S, and G_2-M after prior exclusion of pre-G_1-G_0 events.

Caspase Induction Assay

For detecting the caspase activation, a Promega apoptosis kit was used according to the manufacturer's instructions. Briefly, a caspase-3/7 substrate bis-(*N*-ZBZ-L-aspartyl-L-glutamyl-L-valyl-L-aspartic acid amide) that has been tagged with the fluorescent protein rhodamine-110, was added to glioblastoma cells treated with either QLT0254 or QLT0267 for 72 h. Untreated cells were included as controls. Cleavage of the caspase-3/7 substrate due to endogenous glioblastoma caspase activity results in high fluorescence intensity by rhodamine (excitation, 499 nm). The fluorescence activity of rhodamine is proportional to the amount of caspase-3/7 cleavage and was measured with a FluoStar/PolarStar Optima microplate reader (BMG Lab Technologies).

Nuclear Morphology

Untreated and treated cells were incubated for 72 h in medium at 37°C without additional drug treatment. Cells were then harvested and stained with 0.1 μg/mL 4′,6-diamidino-2-phenylindole (DAPI) for 30 min.

Cells were cytospun onto a glass slide, mounted in 90% glycerol, and viewed under UV light with a Leica DMLB microscope equipped with a ×40 objective lens. Images were captured using Retiga 1300i CCD digital camera and Improvision software.

ELISA Assay of VEGF Levels

U87MG glioblastoma cells transfected with a retroviral construct with a PTEN-inducible promoter (U87.23) were seeded into 100-mm dishes at a density of 2×10^6 per dish and incubated in regular medium overnight then placed in serum-free medium for 24 h. Twenty-four hours later, U87.23 cells were left untreated, treated with muristerone A to induce PTEN, and/or treated with LY294002, QLT0254, or QLT0267. Following 24-h incubation, the conditioned medium was removed and stored at −70°C until VEGF concentration could be determined by ELISA (R&D Systems). U87MG glioblastoma xenograft tumors were

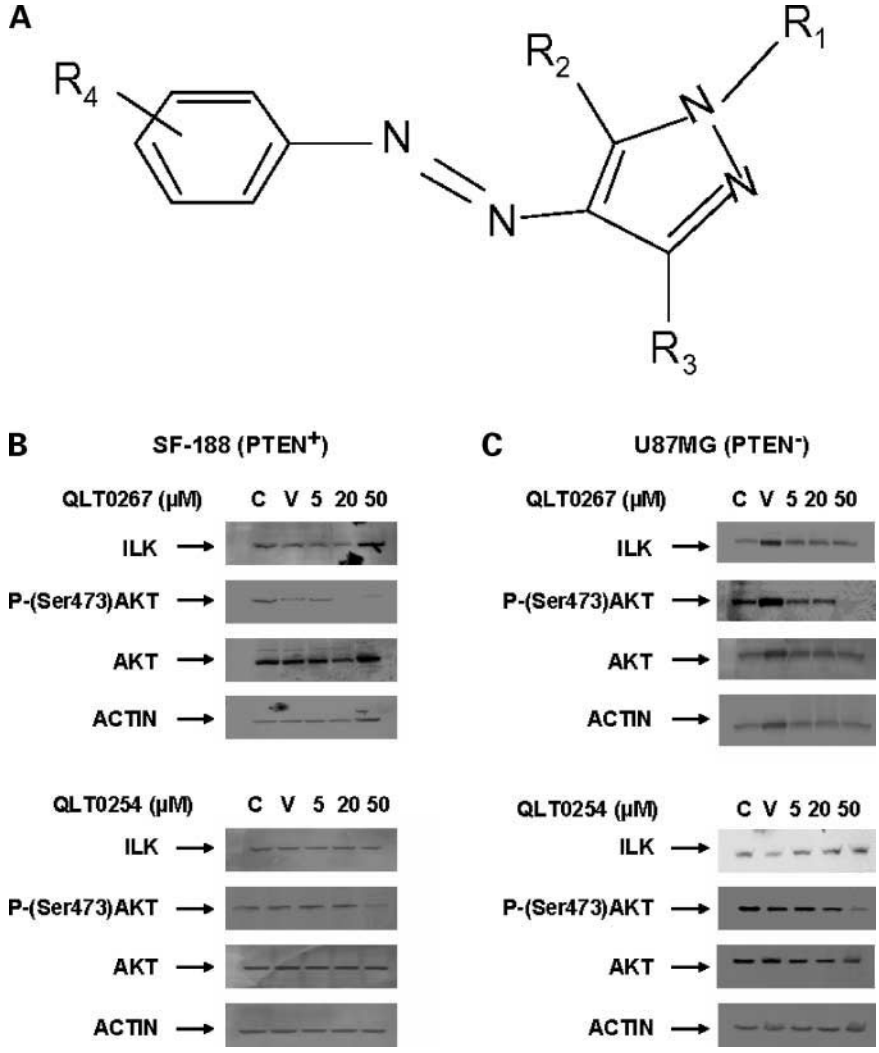

Figure 1. Structure and effects of ILK inhibitors on glioblastoma cell lines. **A**, general structure of ILK inhibitors belonging to the K15792 class of the pharmacor family. **B** and **C**, effects of QLT0254 and QLT0267 on the phosphorylation of the cell survival protein PKB/Akt in glioblastoma SF-188 (**B**) and U87MG (**C**) cells. Cultured cells were incubated with either QLT0267 (**B**, *top*) or QLT0254 (**B**, *bottom*) at drug concentrations of 0, 5, 20, and 50 μmol/L for 48 h. Protein lysates were prepared, and 30 μg of each lysate were resolved by electrophoresis, transferred to membranes, and probed with the indicated antibodies.

homogenized using a mortar and pestle in NP-40 lysis buffer containing complete-mini protease inhibitor cocktail tablet (Roche) and the tumor lysates removed and stored at −70°C until subsequent determination of VEGF concentration as above.

Western Blot Analysis

The following antibodies were used in this study: anti-phospho-Akt- Ser^{473}, anti-ILK, anti-Akt (New England Biolabs); anti-human β-actin (Sigma) anti-HA (Roche), anti-HIF-1α (Santa Cruz Biotechnology), and anti-VEGF (Calbiochem).

The secondary antibody used was horseradish-conjugated anti-mouse or anti-rabbit IgG (Promega). Equivalent amounts of protein (30 μg determined by Bradford assay) were resolved by 4% to 15% gradient SDS-polyacrylamide premade gels (Bio-Rad). Proteins were detected by enhanced chemiluminescence (Amersham Pharmacia Biotech) and visualized after exposure to Kodak autoradiography film. Actin was used as a loading control. Densitometric analysis was done using Quantity one (Bio-Rad Laboratories Ltd.).

Animal Xenograft Models and Antitumor Activity of ILK Inhibitors

Male 129S6/SvEvTac-$Rag2^{tm1Fwa}$ (RAG2-M) mice (7-9 weeks old, 20-27 g) were housed in aseptic environments within the BC Cancer Agency Joint Animal Facility. Efficacy experiments were conducted in mice bearing U87MG tumors (9 or 18 mice per group). Note that the group containing 18 mice was designated as harvesting group, and mice were sacrificed and tumor tissue taken for various analyses (that is, Western blot, immunohistochemistry, and ELISA) at defined time points (that is, day 16). Groups were designed to contain 9 mice for each treatment arm assessing tumor growth. Mice that survived to day 18 were included in the study. Mice were removed from the study if tumors ulcerated or when rapid tumor progression resulted in tumor sizes in excess of 1 g before completion of the treatment course.

The tumor growth results presented are thus based on 6 animals per group in the saline and QLT0267 groups and 7 animals for the PTE vehicle group. Therefore, 6 of 9 mice

survived to day 18 in saline-treated and QLT0267-treated mice. One tumor from PTE vehicle-treated, saline-treated, and QLT0267-treated tumor were removed due to rapid tumor progression. Two tumors from QLT0267 were removed due to tumor ulceration.

One tumor from PTE vehicle was removed due to tumor ulceration. Two tumors from saline-treated tumors were removed due to tumor ulceration. Treatment was initiated when tumors reached at least 5 mm^3. Electronic calipers (Mitutoyo Corp.) were used to measure tumors, and the mean tumor size (mm^3) was determined using the formula: 1 / 2 [length (mm)] $\times$ [width (mm)]^2. The tumor size per mouse was used to calculate the group mean tumor size $\pm$ SE (n = 6 or 7 mice). Saline, the vehicle control PTE PEG_{300}/ethanol/Tween 80/citrate (63:29:7.8:0.2 w/v/w/w), or the ILK inhibitor QLT0267 were administered by oral gavage once a day at a dose of 200 mg/kg for the drug or the corresponding volume for vehicle for the duration of the study.

Fluorescence-Activated Cell Sorting Analysis for Tumor Hypoxia

To measure hypoxia, RAG2-M mice with U87MG xenograft tumors were injected i.p. and i.v. (1:1) with EF-5 solution at 30 mg/kg (a kind gift from Dr. Cameron Koch, University of Pennsylvania) in PBS buffer (137 mmol/L NaCl, 2.7 mmol/L KCl, 10 μmol/L Na_2HPO_4, 2 μmol/L KH_2PO_4), which labels hypoxic cells, 3 h before tumor harvesting of the treated groups and the saline-treated group.

Tumors were disaggregated using a BD Medimachine system (BD Biosciences) and stained with an anti-EF-5 antibody and Cy3 secondary antibody, and flow cytometry was used to visualize and quantify hypoxic tumor cells compared with nonhypoxic tumor cells.

Tumor Vessel Perfusion (Hoechst 33342) and Immunohistochemistry Staining of Tumor Sections for CD31, Bromodeoxyuridine, and EF-5 Labeling

About 3 h before tumor excision, RAG2-M mice were injected with EF-5 as described previously. Hoechst 33342 (100 μL, 16 mg/mL; Sigma-Aldrich) in PBS was injected i.v. 20 min before tumor harvest. Serial tumor cryosections (10 μm thick) were cut with a Cryostar HM560 (Microm International GmbH), air dried for 24 h, then fixed in a 1:1 mixture of acetone-methanol for 10 min at room temperature, and blocked with 3% H_2O_2. Vasculature was stained using CD31 antibody (1:100 dilution; BD PharMingen) and Alexa 546 goat anti-rat secondary antibody (1:50 dilution; Molecular Probes). Some tumor sections were fixed with ice-cold acetone for 5 min, air-dried, and stained with ELK3-51-CY3 antibody to detect EF-5 adducts according to procedures described elsewhere (25). Slides then were mounted with PBS and imaged (see Image Acquisition). Note that separate sections were used for EF-5 staining in contrast to the same sections used for CD31 and Hoechst 33342 staining.

About 2 h before tumor harvesting, mice were injected i.p. with 30 mg/mL solution of bromodeoxyuridine (BrdUrd; Sigma). After imaging for Hoechst and CD31, slides were rinsed in PBS, placed in distilled water for 10 min, and treated with 2 mol/L HCl at room temperature for 1 h followed by neutralization for 5 min in 0.1 mol/L sodium borate. Slides were washed in distilled water and transferred to a PBS bath. Subsequent steps were each followed by a 5-min wash in PBS. Incorporated BrdUrd was detected using a monoclonal mouse anti-BrdUrd antibody (1:200 dilution, clone BU33; Sigma) followed by an anti-mouse peroxidase conjugate antibody (1:100 dilution; Sigma) and a metal enhanced diaminobenzidine substrate (1:10 dilution; Pierce). All slides were counterstained with hematoxylin, dehydrated, and mounted using Permount (Fisher Scientific) before imaging.

Image Acquisition

Images were captured using a fluorescence microscope (III RS; Zeiss) with a cooled monochrome charge-coupled device video camera (model 4922; Cohu), frame grabber (Scion), a custom-built motorized x-y stage, and customized NIH Image software[10] running on a G4 Macintosh computer (Apple).

Slides with tumor sections were imaged for Hoechst 33342 fluorescence using a 360 nm excitation and a 450 nm long-pass emission filters, and the same slides were imaged for CD31-Alexa 546; these slides were finally imaged for BrdUrd and hematoxylin in a bright field. Acquired images were stacked and a composite color image of CD31/Hoechst 33342, EF-5, and BrdUrd were produced by adding the grayscale BrdUrd/tissue layer or, in some cases, pseudo-colored with Adobe Photoshop according to tissue layer.

Image Analysis of Hoechst 33342, EF-5, CD31, and BrdUrd Staining

The NIH Image software application and algorithms were generously provided by Dr. Andrew Minchinton (BC Cancer Agency). Tumor tissue sections were analyzed in viable tissue areas identified based on hematoxylin staining. Staining artifacts were removed from analysis. Hoechst 33342–positive regions were identified by selecting all pixels that were 12 SDs above the tissue background. For CD31 and BrdUrd images, positive staining was selected as pixels that were 5 or 2.5 SD above background levels, respectively. Threshold levels were kept constant for all analysis. $CD31^+$ regions that were <5 μm^2 in size were considered artifacts and removed from the analysis. The fraction of perfused (functional) vessels was determined by comparing CD31 and Hoechst 33342 labeling of vasculature; $CD31^+$ vessels were considered perfused if >2% of pixels of each $CD31^+$ object were also Hoechst 33342 positive.

This estimation of blood vessel function was dependent on the time point evaluated after Hoechst 33342 injection. The percentage of CD31 and BrdUrd was defined as the number of positive pixels over the total number of pixels in viable tissue. Note that for all analysis (except for EF-5 labeling where four tumors were evaluated for both control and treated groups) of CD31, BrdUrd, and Hoechst 33342 stained tumor sections were evaluated based on an n of at least 5 for treatment and control arms of the study.

[10] http://rsb.info.nih.gov/nih-image/

Statistical Analysis

All of the statistical analyses were done using the Statistica program. Data analysis for multiple comparisons of treatment and control groups was done using the ANOVA Tukey test. Data were considered significant for $P < 0.05$.

Results

QLT0254 and QLT0267 Inhibit Growth of Selected Glioblastoma Cells *In vitro*

SF-188 (PTEN-positive) and U251MG and U87MG (PTEN-negative) glioblastoma cells were treated with increasing concentrations of the ILK inhibitor QLT0254 or QLT0267 for 48 h, and a 3-(4,5-dimethylthiazol-2-yl)-2,5-diphenyl tetrazolium bromide (MTT) assay was used to determine growth inhibition. Treatment with either ILK inhibitor for 48 h reduced MTT labeling compared with controls indicative of cell cytotoxicity and/or cell cytostasis of all cell lines tested.

The values from the MTT assay were analyzed by the software program Calcusyn to determine the IC_{50}s (Supplementary Table S1)[11] for the individual agents.

QLT0254 and QLT0267 Inhibit PKB/Akt Activity in Selected Glioblastoma Cells

Several studies have shown that using PTEN-transfected cells, cells expressing a dominant-negative ILK, an ILK antisense, or small interfering RNA targeting ILK, results in ILK inhibition that subsequently affects the phosphorylation and activation of PKB/Akt at Ser^{473}, a well-known cell survival signaling protein (26–28). Therefore, we investigated if two small-molecule inhibitors from the K15792 class of the pharmacophor family (Fig. 1A), QLT0254 and QLT0267, could decrease phosphorylation of PKB/Akt. The results are summarized in Fig. 1B and C. Glioblastoma SF-188 and U87MG cells exposed to QLT0267 showed loss of phospho-PKB/Akt at Ser^{473} (Fig. 1B and C, *top*). Cells treated with QLT0254 (Fig. 1B and C, *bottom*, respectively) exhibited partial loss of phospho-PKB/Akt at Ser^{473} at 50 μmol/L. Similar results for both inhibitors were also seen in the glioblastoma U251MG cell line also (data not shown). Note that treatment with the QLT0254 and QLT0267 ILK inhibitors did not affect ILK protein expression. Total PKB/Akt was also unaffected by these inhibitors.

Effects of QLT0254 and QLT0267 on Cell Cycle Regulation in Selected Glioblastoma Cell Lines

To determine the effects of ILK inhibition on cell cycle distribution in U251MG, SF-188, and U87MG cells, the cells were treated with QLT0254 or QLT0267 at concentrations ranging from 0 to 50 μmol/L for a maximum of 24 h and analyzed within 12 to 24 h after treatment for DNA content with propidium iodide staining and flow cytometry. The results in Fig. 2 indicated that SF-188 cells treated with QLT0267 appear to have a significant buildup in the S phase of the cell cycle indicative of a cell cycle delay or block (Fig. 2A, *left*). Cells treated with QLT0254 (U87MG) or QLT0267 (U251MG) exhibited a strong, dose-dependent, G_2-M block. PTEN-negative U251MG cells showed considerable G_2-M block when treated with 20 or 50 μmol/L QLT0267 (Fig. 2A, *middle*). Similar effects were noticed when U251MG cells were treated with QLT0254 (data not shown). PTEN-negative U87MG cells were blocked in G_2-M following treatment with QLT0254 at 20 or 50 μmol/L (Fig. 2A, *right*). Similar results were observed for U87MG cells treated with QLT0267 (data not shown).

Induction of Apoptosis following Treatment with QLT0254 and QLT0267

To assess whether ILK inhibition by QLT0254 and QLT0267 could induce apoptosis, the activity of caspase-3 and/or -7 was assessed. The different cell lines were exposed to 5 or 20 μmol/L QLT0254 or QLT0267, drug concentrations that were typically less than the IC_{50} (see Supplementary Table S1).[11]

Because cell cycle arrest was observed within 1 day following treatment with QLT0254 and QLT0267, apoptosis was assessed following longer incubation times (72 h with drug). Representative data for SF-188 and U251MG cell lines treated with QLT0267 and the U87MG cell line treated with QLT0254 are provided in Fig. 2B. Caspase activity significantly increased for SF-188 (Fig. 2B, *far left*), U251MG (Fig. 2B, *middle*), and U87MG (Fig. 2B, *far right*) following exposure to the ILK inhibitors. No significant changes in caspase activity compared with controls were observed for cells treated with PTE vehicle or when using the ILK inhibitors at 5 μmol/L (Fig. 2B). These data suggest that QLT0254 and QLT0267 can induce caspase activation.

Apoptosis with QLT0254 and QLT0267 drug was also confirmed with DAPI staining. Numbers of fragmented and condensed nuclei (Fig. 2C, *micrographs*), indicative of apoptosis, were recorded and expressed as a fold increase relative to untreated controls (Fig. 2C, *bar graphs*). SF-188 (*far left*) and U251MG (*middle*) cells treated with QLT0267 and also U87MG cells (*far right*) treated with QLT0254 exhibited a significant increase in apoptotic cells shown by DAPI when compared with untreated and vehicle-treated controls.

Regulation of VEGF Secretion by ILK in U87.23 Glioblastoma Cells

It has been shown that VEGF in glioblastomas is regulated in a PI3K-dependent manner (29).

To determine if ILK inhibition could inhibit VEGF secretion, we used PTEN-negative U87MG glioblastoma cells transfected with an ecdysone-inducible (30) wild-type PTEN retroviral construct (designated here as U87.23). The ecdysone-inducible expression system allows the expression of the PTEN gene in the presence of muristerone A. A concentration of 0.5 μmol/L muristerone A allows for the full expression of PTEN (Fig. 3, *gel*). An ELISA assay was used to assess secreted VEGF levels in cells exposed to muristerone A or the ILK inhibitors and these data are summarized in Fig. 3. Uninduced U87.23 glioblastoma cells (PTEN-negative) showed high secreted VEGF protein levels (Fig. 3, *bar graph*). On

[11] Supplementary material for this article is available at Molecular Cancer Therapeutics Online (http://mct.aacrjournals.org/).

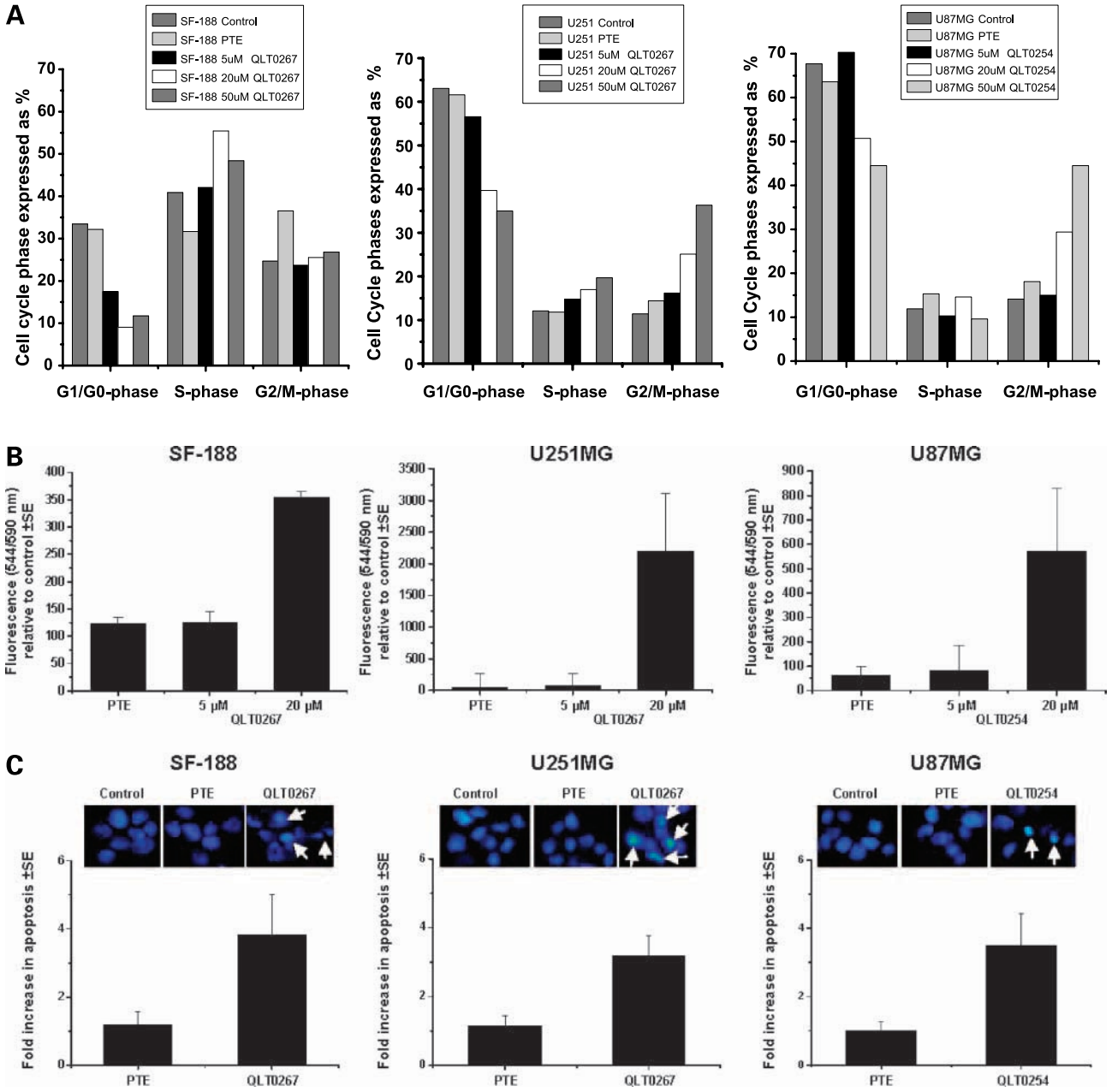

Figure 2. *In vitro* assessment of cell cycle and apoptosis following treatment with the ILK inhibitors. **A,** cultured cells were treated for 24 h with QLT0254 or QLT0267 at the indicated concentrations. A breakdown of the cell cycle phases indicates a S-phase block for SF-188 (**A**, *left*) and a dose-dependent G_2-M-phase block in U251MG (**A**, *middle*) and U87MG (**A**, *right*). Representative experiments. **B,** caspase activation in SF-188 (**B**, *left*), U251MG (**B**, *middle*), and U87MG (**B**, *right*) with increasing concentrations of ILK inhibitors incubated with glioblastoma cells for 72 h. Mean of six replicates; *bars,* SE. Representative of two independent experiments. Data are expressed relative to values obtained from untreated control cells. **C,** glioblastoma cells were untreated or incubated with PTE (vehicle control) or 20 μmol/L QLT0254 or QLT0267 for 72 h and then stained with 4′,6-diamidino-2-phenylindole. Morphologic features of cellular apoptosis were observed with a fluorescence microscope. Representative images of cells stained with 4′,6-diamidino-2-phenylindole. *Arrows,* apoptotic cells with condensed chromatin. Representative images. Fold increase (*bar graphs*) was determined scoring five random fields for each condition, and the scoring was done in a blinded fashion. Data are expressed relative to untreated control cells as mean ± SE.

induction of PTEN by exposure to 0.5 μmol/L muristerone A, secreted VEGF levels decreased 3-fold. Exposure of uninduced U87.23 glioblastoma cells to the ILK inhibitors QLT0254 or QLT0267 also resulted in significant decreases in secreted VEGF levels. As an additional positive control, exposure of U87.23 glioblastoma cells to LY294002, the inhibitor of PI3K, resulted in a similar decrease in VEGF secretion.

Antitumor Efficacy of QLT0267 in U87MG Tumor Xenografts

Because QLT0267 has not been tested in an *in vivo* model of glioma, we decided to test the antitumor effects of this ILK inhibitor (QLT0267) in RAG2-M mice bearing s.c. xenografts derived following injection of PTEN-negative U87MG glioblastoma cells (Fig. 4).

Mice were treated with either saline, QLT0267, or PTE vehicle; the drug was dosed orally at 200 mg/kg (see Materials and Methods) and PTE was administered at a volume and dose equivalent to that used in the formulated drug product. Treatment commenced 32 days after initial tumor injection when the tumor size was measurable. Mice that survived to day 18 post-treatment initiation were included in the study; mice within each group were removed from the study if they ulcerated or if tumor sizes were in excess 1 g before completion of the full treatment schedule. Saline-treated or PTE (vehicle)–treated animals exhibited tumors that grew reproducibly to an average size of 0.8 cm^3 within 18 days of treatment initiation. Treatment with vehicle alone did not cause any significant change in tumor growth rate when compared with the saline control. Comparing the saline-treated animals with the QLT0267-treated animals, the tumor size in the QLT0267-treated groups was significantly smaller. On day 16, for example, tumors from mice treated with QLT0267 were 213 mm^3 versus 549 mm^3 in control mice (difference, 336 mm^3; 95% CI, 304-794 mm^3; $P < 0.001$) post-treatment. Significant decreases in tumor volume were noted on day 18 for tumors in treated mice compared with controls (Fig. 4, *insets*). Animals treated with QLT0267 exhibited a mean tumor volume of 292 mm^3 compared with tumors from control animals that were on average 770 mm^3 (difference, 478 mm^3; 95% CI, 624-916 mm^3; $P < 0.001$). These results suggested that QLT0267 was therapeutically active *in vivo*.

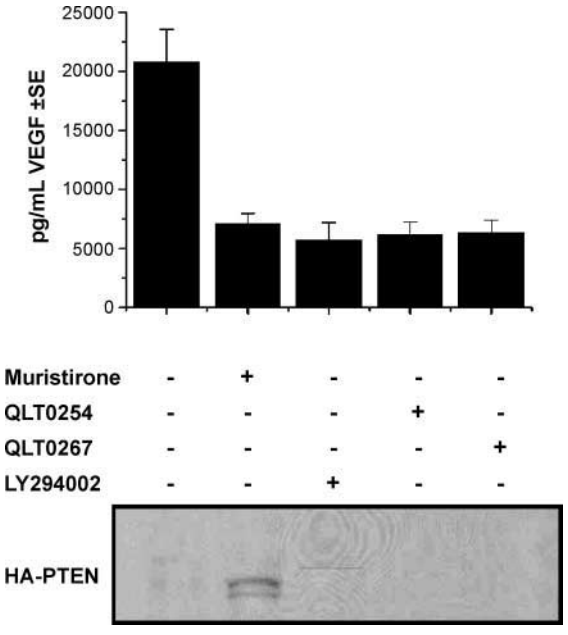

Figure 3. ILK inhibition results in suppression of VEGF secretion. PTEN in U87.23 cells were induced with muristerone A or treated with QLT0254, QLT0267 (20 μmol/L), or LY294002 (20 μmol/L). After 24 h, supernatants were collected and VEGF protein levels were determined by ELISA. Representative of four separate experiments. Western blot analysis was used to analyze PTEN expression in U87.23 cells treated with different agents.

Further, the results clearly suggest that ILK inhibition with QLT0267 caused a delay in tumor growth in this model, which is also shown by individual mouse growth curves for inset graphs for PTE-treated (Fig. 4, *top left*) and QLT0267-treated (Fig. 4, *top right*) animals. None of the mice treated with QLT0267 displayed signs of toxicity in general; specifically, the 200 mg/kg dose given once a day resulted in less than 5% body weight loss.

ILK Inhibition by QLT0267 Results in Decreased Hypoxia, Suppression of VEGF and HIF-1α Expression, and Cell Proliferation

To investigate further biological effects of ILK inhibition, we focused our *in vivo* analyses on QLT0267, which we have shown to be therapeutically active (Fig. 4). Serial tumor tissue sections were generated from PTEN-negative U87MG tumors from animals treated with either saline or QLT0267. Sections were imaged for Hoechst 33342 (as a perfusion marker) and stained with ELK3-51-CY3 antibody (anti-EF-5-CY3 used to stain for cells labeled with EF-5) and another serial section from the same tumor was imaged for Hoechst 33342 and stained for tumor vascular endothelial cells with anti-CD31 antibody. Representative photomicrographs are shown in Fig. 5A. Control tumors from saline-treated mice show substantial EF-5 labeling indicative of hypoxia in viable tissue of control tumors (Fig. 5A). It is notable that EF-5 labeling was most frequently observed in regions that showed reduced Hoechst 33342 labeling (less perfused vasculature).

Tumors from QLT0267-treated animals showed reduced CD31 staining and reduced Hoechst 33342 vessel perfusion (primarily localized to the periphery of the section) compared with control tumors. An initial quantitative analysis of EF-5 staining appeared to show a decrease in hypoxia (Fig. 5A, *histogram*); therefore, an alternate approach using ILK antisense versus saline-treated U87MG xenograft tumors was used to verify the effects of ILK inhibition on hypoxia (see Materials and Methods). Harvested and disaggregated EF-5-labeled tumors were labeled with anti-EF-5-CY3 antibody and analyzed by fluorescence-activated cell sorting (Fig. 5B). The level of hypoxia in saline-treated tumors was nearly double that of tumors treated with an ILK antisense, providing further evidence that ILK inhibition results in decreased hypoxia.

The *in vitro* results show that QLT0267 engenders a reduction in cell proliferation and lower VEGF expression; for this reason, these endpoints were also used to assess the activity of QLT0267 *in vivo* in U87MG xenografts. To verify that ILK inhibition affects VEGF protein production *in vivo*, an ELISA assay was used to assess VEGF levels in U87MG

tumor lysates prepared from tumors isolated from RAG2-M mice treated with QLT0267 or saline. As shown in Fig. 5C (*bar graph*), a 50% decrease in measurable VEGF was observed in tumors obtained from animals treated with QLT0267 at 200 mg/kg.

These data are consistent with *in vitro* data (Fig. 3) and clearly indicate that QLT0267 inhibits VEGF production in glioblastoma U87MG cells and tumors. We also confirm a decrease in VEGF protein levels in U87MG tumors derived from QLT0267-treated animals with Western blot analysis (Fig. 5C, *gel*). Because it is known that ILK can control VEGF expression by stimulating HIF-1α through a PI3K-dependent activation of PKB/Akt (31, 32), we compared HIF-1α protein levels in lysates prepared from QLT0267-treated and control tumors by Western blotting. The results (Fig. 5C) suggested that HIF-1α levels decreased in QLT0267-treated tumors.

Effects of QLT0267 Treatment on Vasculature of Glioblastoma U87MG Tumor Xenografts

Analysis of tumors from treated animals suggested that ILK inhibition was associated with decreases in hypoxia, VEGF levels, and HIF-1α expression (Fig. 5B and C). Because VEGF and HIF-1α are known to stimulate angiogenesis (33), we focused our remaining analysis on establishing how QLT0267 affected tumor vascularization. Representative images of U87MG xenograft tumor sections isolated from animals treated with saline or QLT0267 and perfused *in vivo* with Hoechst 33342 (*light blue*) are shown in Fig. 6A (saline-treated) and Fig. 6B (QLT0267-treated).

Details showing tumor vasculature either stained with anti-CD31 antibody alone (indicative of nonfunctional tumor vessels; *red*) or stained with anti-CD31 antibody and Hoechst 33342 (Hoechst 33342 perfusion indicates that

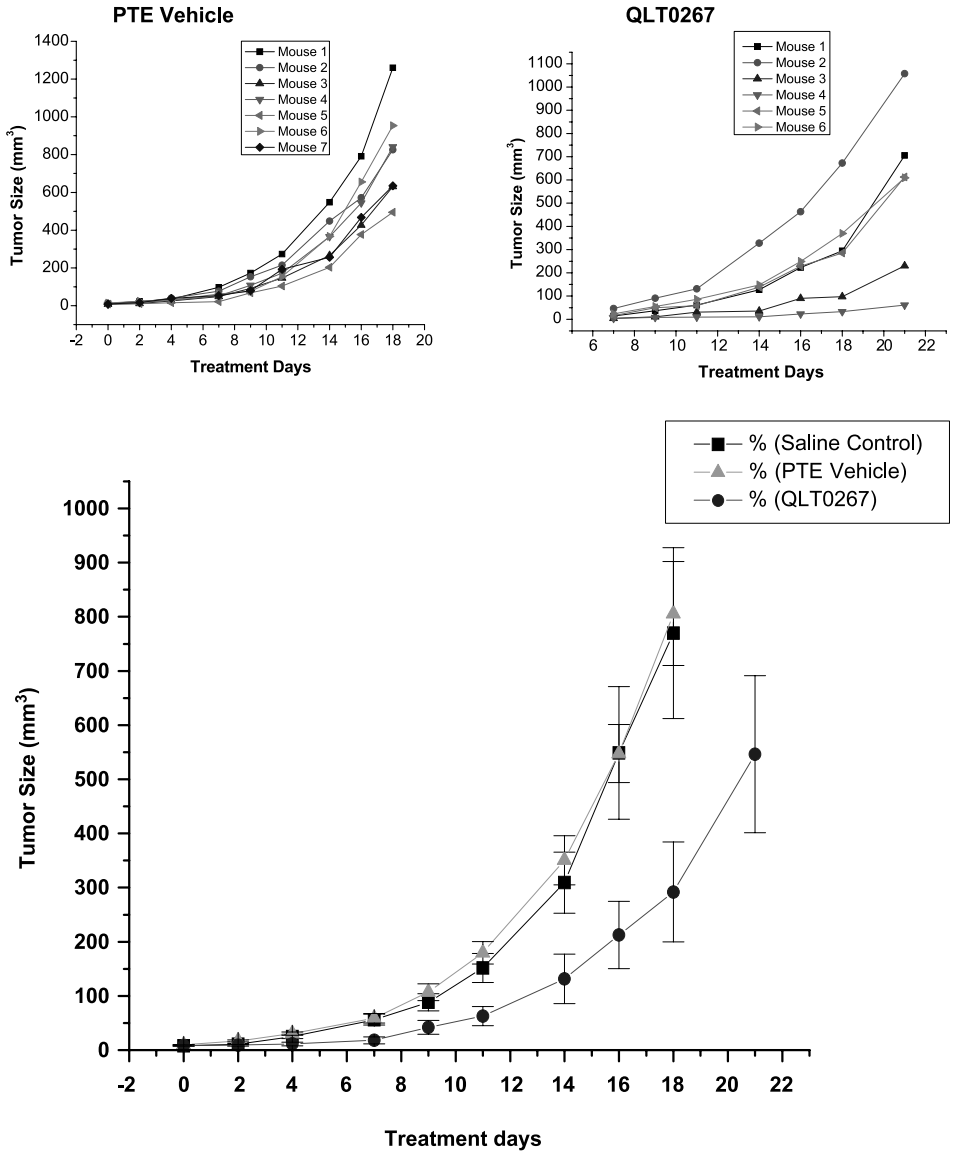

Figure 4. Efficacy of QLT0267 in U87MG glioblastoma xenografts. A comparison of tumor volume among the two treatment groups and control. RAG2-M mice bearing U87MG xenograft tumors were orally dosed with either saline, PTE (vehicle), or QLT0267 at 200 mg/kg q.d. × 7 for 3 wk. Mice that survived to day 18 were included in the analysis. Average tumor volumes ± SE for $n = 6$ mice in the saline vehicle and QLT0267 groups and $n = 7$ mice in the PTE vehicle groups. *Inset,* individual mouse growth curves of PTE vehicle group (*top left*) and QLT0267 group (*top right*) to day 18 post-treatment.

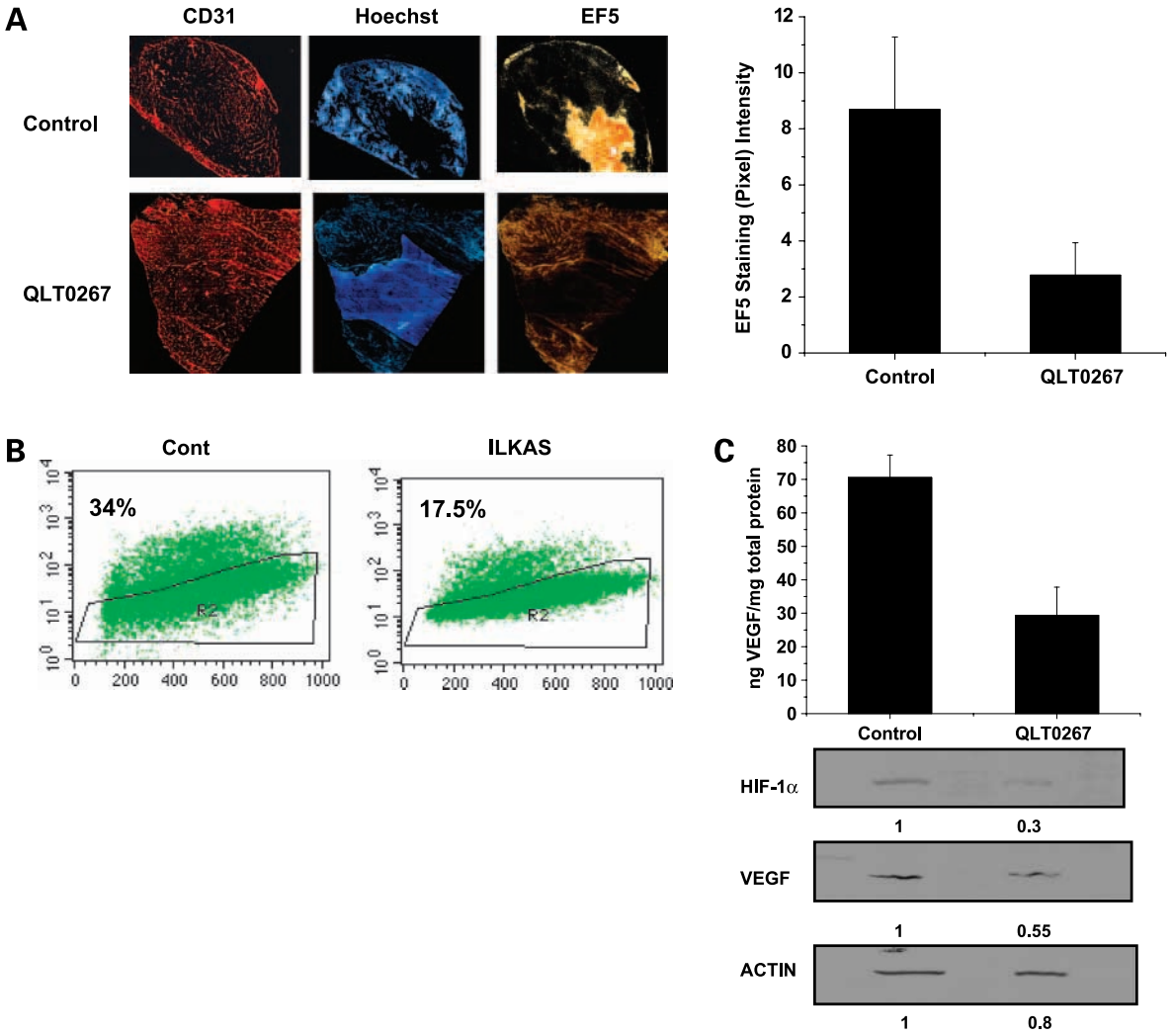

Figure 5. Effects of QLT0267 on hypoxia, VEGF, HIF-1α protein levels in U87MG tumors. **A,** examination of hypoxia in glioblastoma xenografts. Tumor tissues were taken day 16 post-treatment. Representative serial sections of U87MG xenograft tumors stained with PECAM/CD31 antibody (*left, red*) and Hoechst 33342 (*middle, blue*) or anti-EF-5-CY3 antibody (*right, orange/yellow gold* not in the same section). EF-5 (*orange/yellow gold*) staining is used to assess the hypoxic fraction of the tumor (*top right*). **B,** quantitative analysis of EF-5 labeling by fluorescence-activated cell sorting reveals ILK inhibition by an ILK oligonucleotide showing a significant decrease in hypoxia compared with control tumors (34% versus 17.5%). **C,** tumor lysates were collected from saline-treated or QLT0267-treated (200 mg/kg) animals. VEGF protein levels were determined by ELISA. *Columns,* mean of three separate experiments, each one including three different tumor lysates; *bars,* SE (*top*). *, $P < 0.05$. Western blot analysis of VEGF and HIF-1α expression in lysates derived from U87MG tumors harvested from control and QLT0267-treated animals (*bottom gel*). *Numbers below each band,* densitometric analysis where the proteins under investigation were normalized to the saline-treated control lane = 1.

CD31$^+$ vessels are functional; *light blue-red/purple*) are shown in the enlarged images in Fig. 6A and B. To measure and compare tumor cell proliferation in the tumors of animals treated with QLT0267 or saline, BrdUrd was used as a label (*black dots*). There is clearly more BrdUrd label in saline-treated tumors than in QLT0267-treated tumors (Fig. 6A and B, *enlarged images*). Quantitative analyses of all images are summarized in Fig. 6C and are described in Materials and Methods. BrdUrd analysis revealed a decrease in cell proliferation with QLT0267-treated tumors compared with saline-treated tumors (Fig. 6C, *left*). CD31$^+$ and CD31$^+$/Hoechst 33342–positive pixels were quantitated in viable tumor tissue; the results indicated that vessel mass (% CD31$^+$ pixels) was decreased following QLT0267 treatment compared with saline-treated control tumors (Fig. 6C, *middle*). In addition, the proportion of CD31$^+$ vessels that were Hoechst 33342 perfused was significantly lower in tumors from animals treated with QLT0267 when compared with saline-treated animals (Fig. 6C, *right*).

Discussion

ILK inhibition has been evaluated as a treatment strategy in a number of animal models of cancers (19, 20, 34–36). It is

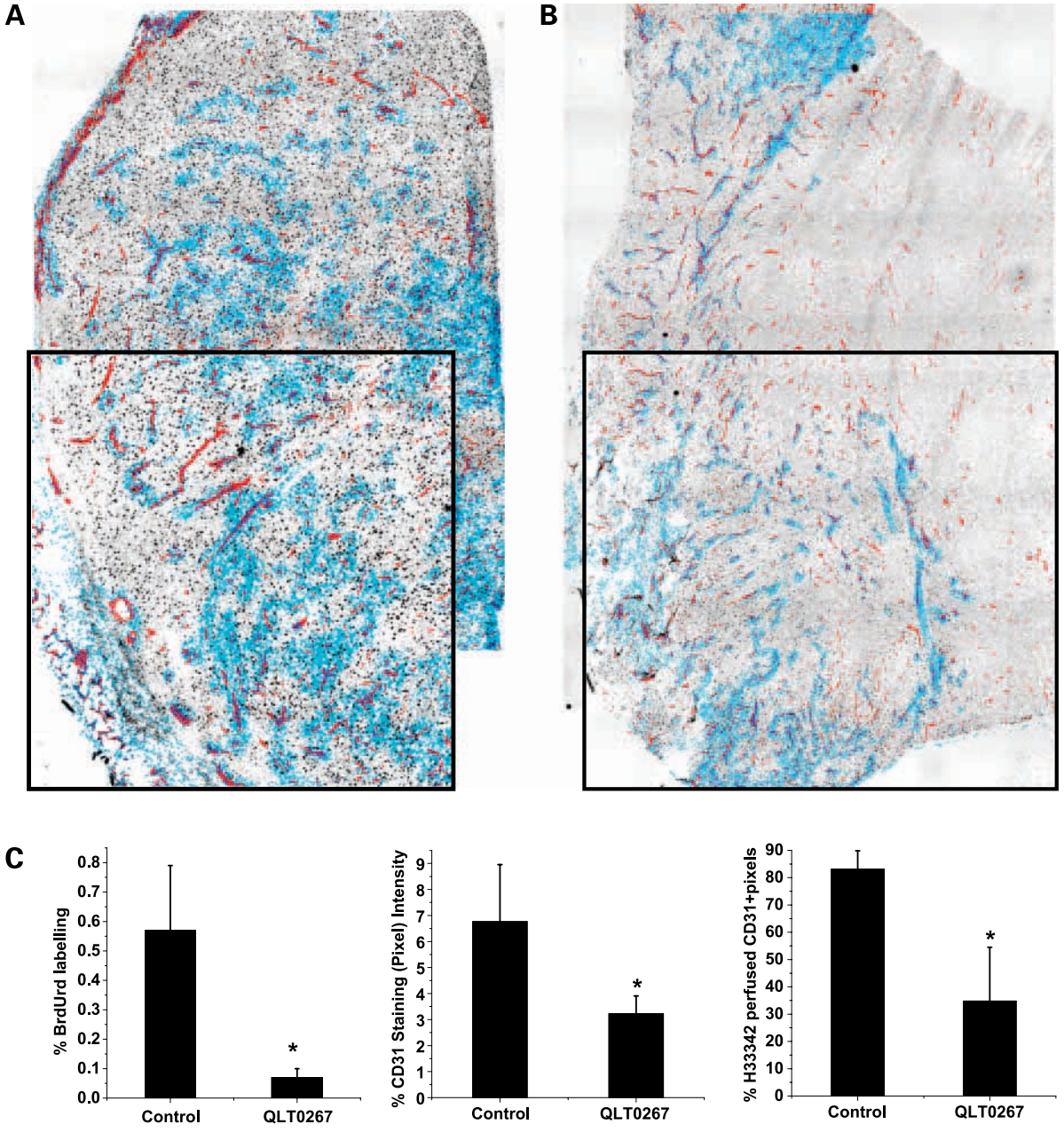

Figure 6. Analysis of vasculature in U87MG tumors. **A** and **B,** images of frozen tumor tissue sections from representative saline-treated (**A**) and QLT0267-treated (**B**) U87MG tumors perfused *in vivo* with Hoechst 33342 (*light blue*) and stained with CD31 antibody (*red*). **C,** *left,* percentage of BrdUrd-positive viable tumor tissue in saline-treated and QLT0267-treated tumors (mean ± SE, $n = 6$). *, $P < 0.01$. *Middle,* percentage of CD31-stained viable tumor tissue in QLT0267-treated tumors compared with controls (mean ± SE; $n = 6$). *, $P < 0.028$. *Right,* percentage of $CD31^+$ pixels that are also positive for Hoechst 33342 in viable tumor tissue in QLT0267-treated tumors compared with saline-treated controls (mean ± SE; $n = 6$). *, $P < 0.01$.

apparent from these previous studies that ILK inhibition slows down the rate of tumor growth, but inhibition using the current generation of ILK inhibitors does not appear to affect a reduction in tumor size. It is important from a mechanistic perspective to gain a better understanding of how ILK inhibition inhibits tumor growth *in vivo*. In particular, ILK is a therapeutic target that if inhibited could cause (*a*) a reduction in tumor cell proliferation, (*b*) an induction of apoptosis, and/or (*c*) inhibition of VEGF secretion. The results summarized here suggest that QLT0267 exerts some activity on each of these independent endpoints.

Interestingly, the ILK inhibitors appeared to be more sensitive toward the PTEN-positive cell line. The presence

of PTEN in cells contributes to a lower baseline of ILK and Akt activity; therefore, it is reasonable that ILK inhibition would result in more pronounced effects in active PTEN-positive cells. This can be seen in Fig. 1B with the PTEN-positive SF-188 cells where phospho-Akt activity is knocked down at a concentration of 20 μmol/L. Our data show that QLT0254 and QLT0267 were therapeutically effective *in vitro*. In addition to growth inhibition, both of these ILK inhibitors suppressed expression of phospho-PKB/Akt at Ser^{473} and lowered *in vitro* levels of VEGF produced by glioblastoma cells.

Similarly, other investigators also showed that *in vitro* treatment of glioma cells with QLT0267 blocked phosphorylation of Akt and its downstream targets and inhibited cell growth (20). Our data also suggest that decreased VEGF secretion was mediated by the ILK inhibitors and this decrease was comparable with decreases associated with induction of PTEN. Further, we show that QLT0267 and QLT0254 induced a S-phase or G_2-M block (cytostatic effects) and apoptotic cell death (cytotoxic effects). The difference in cell cycle profiles, we believe, was due to differences in PTEN status. S-phase block occurred in PTEN-positive cells and translated to cell cycle arrest that was not followed by a large increase in cell death with longer exposure of drug treatment compared with PTEN-negative cell lines where G_2-M block and cell death could be seen with longer drug exposure.

To characterize the *in vivo* mechanism of action for the ILK inhibitor QLT0267, we focused on several therapeutically interesting endpoints. Through this analysis, we determined that ILK inhibition by QLT0267 is associated with a considerable decrease in tumor cell proliferation, inhibition of VEGF and HIF-1α, and a decreased percentage of CD31 staining in viable tumor tissue, indicative of a decline in microvessel mass, accompanied by a decrease in Hoechst 33342 perfused functional microvessels. Based on these data, we believe that QLT0267 acts as an antiproliferative, antiangiogenic, and antivascular agent *in vivo*.

Our results agree with the published study of Younes et al. who similarly found inhibition of the tumor vasculature in anaplastic thyroid cancer after treatment of xenografts with QLT0267 (19).

Our study highlights the benefit of using a targeted agent that inhibits a kinase within a central pathway known to affect cell survival, cell proliferation, and angiogenesis. We believe that analyzing multiple therapeutic endpoints, such as cell proliferation and apoptosis together with molecular alterations in survival and angiogenic pathways in addition to analysis of treatment-associated changes in the tumor microenvironment such as tumor vascularization and perhaps hypoxia, will improve the veracity of therapeutic approaches based on rational drug targets and will be especially helpful in designing effective combination treatments. Whether the anticancer properties of QLT0267 shown in this preclinical study will translate into clinically meaningful effects in patients can only be determined in the clinical setting.

Acknowledgments

We thank Dr. Mike Wigler and Linda Rogers (Cold Spring Harbor) for their generous contribution of the U87 cells with the vector constructs, The Workers Compensation Board for microscope facilities, the animal care technicians of Advanced Therapeutics for assisting in all the animal studies and tissue culture, and QLT/Kinetek Pharmaceuticals for providing the small-molecule ILK inhibitors and assisting in the design of these studies and assessment of the data resulting from this study.

References

1. Blume-Jensen P, Hunter T. Oncogeneic kinase signaling. Nature 2001; 411:355 – 65.

2. Arteaga CL, Baselag J. Tyrosine kinase inhibitors: why does the current process of clinical development not apply to them? Cancer Cell 2004;5: 525 – 31.

3. Brown I, Giaccia AJ. Tumor hypoxia: the picture has changed in the 1990's. Int J Radiat Biol 1994;65:95 – 102.

4. Semenza GL. Hypoxia, clonal selection, and the role of HIF-1 in tumor progression. Crit Rev Biochem Mol Biol 2000;35:71 – 103.

5. Forsythe JA, Jiang BH, Iyer NV, et al. Activation of vascular endothelial growth factor gene transcription by hypoxia-inducible factor 1. Mol Cell Biol 1996;16:4604 – 13.

6. Plate KH, Breier G, Weich HA, Risau W. Vascular endothelial growth factor is a potential tumour angiogenesis factor in human gliomas *in vivo*. Nature 1992;359:845 – 8.

7. Mottram JC. Factor of importance in radiosensitivity of tumors. Br J Radiol 1936;9:606 – 14.

8. Tannock I. Response of aerobic and hypoxic cells in a solid tumor to Adriamycin and cyclophosphamide and interaction of the drugs with radiation. Cancer Res 1982;42:4921 – 6.

9. Lee AV. Location, location, location: regulation of breast cancer progression by the microenvironment. Breast Cancer Res 2004;6:279 – 80.

10. Kerr DJ. Targeting angiogenesis in cancer: clinical development of bevacizumab. Nat Clin Pract Oncol 2004;1:39 – 43.

11. Folkman J. Antiangiogenic gene therapy. Proc Natl Acad Sci U S A 1998;95:9064 – 6.

12. Fang J, Zhou Q, Liu L-Z, et al. Apigenin inhibits tumor angiogenesis through decreasing HIF-1 and VEGF expression. Carcinogenesis 2006;28: 858 – 64.

13. Tan C, Cruet-Hennequart S, Troussard A, et al. Regulation of tumor angiogenesis by integrin-linked kinase (ILK). Cancer Cell 2004;5:79 – 90.

14. Hannigan GE, Leung-Hagesteijn C, Fitz-Gibbon L, et al. Regulations of cell adhesion and anchorage-dependent growth by a new β1-integrin-linked protein kinase. Nature 1996;379:91 – 6.

15. Radeva G, Petrocelli T, Behrend E, Leung-Hagesteijn C, Filmus Slingerland J, Dedhar S. Overexpression of the integrin-linked kinase promotes anchorage-independent cell cycle progression. J Biol Chem 1997;272:13937 – 44.

16. Attwell S, Roskelley C, Dedhar S. The integrin-linked kinase (ILK) suppresses anoikis. Oncogene 2000;19:3811 – 5.

17. Edwards L, Thiessen B, Dragowska WH, Daynard T, Bally MB, Dedhar S. Inhibition of ILK in PTEN-mutant human glioblastomas inhibits PKB/Akt activation, induces apoptosis, and delays tumor growth. Oncogene 2005; 24:3596 – 605.

18. Obara S, Nakata M, Takeshima H, et al. Integrin-linked kinase (ILK) regulation of the cell viability in PTEN mutant glioblastoma and *in vitro* inhibition by the specific COX-2 inhibitor NS-398. Cancer Lett 2004;208: 115 – 22.

19. Wang SI, Puc J, Li J, et al. Somatic mutations of PTEN in glioblastoma multiforme. Cancer Res 1997;57:4183 – 6.

20. Koul D, Shen R, Bergh S, et al. Targeting integrin-linked kinase inhibits Akt signaling pathways and decreases tumor progression of human glioblastoma. Mol Cancer Ther 2006;4:1681 – 8.

21. Yau CYF, Wheeler JJ, Sutton KL, Hedley DW. Inhibition of integrin-linked kinase by a selective small molecule inhibitor, QLT0254, inhibits the PI3K/PKB/mTOR, Stat3, and FKHR pathways and tumor growth, and enhances gemcitabine-induced apoptosis in human orthotopic primary pancreatic cancer xenografts. Cancer Res 2005; 65:1497 – 504.

22. Younes MN, Kim S, Yigitbasi OG, et al. Integrin-linked kinase is a

potential therapeutic target for anaplastic thyroid cancer. Mol Cancer Ther 2005;4:1146 – 56.

23. Trousard AA, McDonald PC, Wederell ED, et al. Preferential dependence of breast cancer cells versus normal cells on integrin-linked kinase for protein kinase B/Akt activation and cell survival. Cancer Res 2006;66:393 – 403.

24. Chou T-C, Talalay P. Analysis of combined drug effects: a new look at a very old problem. Trends Pharmacol Sci 1983;4:450 – 4.

25. Evans SM, Joiner B, Jenkins WT, Laughlin KM, Lord EM, Koch CJ. Identification of hypoxia in cells and tissues of epigastric 9L rat glioma using EF5 [2-(2-nitro-1H-imidazol-l-yl)-*N*-(2,2,3,3,3-pentafluoropropyl) acetamide]. Br J Cancer 1995;72:875 – 82.

26. Persad S, Attwell S, Gray V, et al. Inhibition of integrin-linked kinase (ILK) suppresses activation of protein kinase B/Akt and induces cell cycle arrest and apoptosis of PTEN-mutant prostate cancer cells. Proc Natl Acad Sci U S A 2000;97:3207 – 12.

27. Brunet A, Bonni A, Zigmond MJ, et al. Akt promotes cell survival by phosphorylating and inhibiting a forkhead transcription factor. Cell 1999; 96:857 – 68.

28. Zhou H, Li X-M, Meinkoth J, Pittman RN. Akt regulates cell survival and apoptosis at a postmitochondrial level. JCB 2000;151: 483 – 94.

29. Maity A, Pore N, Lee J, Solomon D, O'Rourke DM. Epidermal growth factor receptor transcriptionally up-regulates vascular endothelial growth factor expression in human glioblastoma cells via a pathway involving phosphatidylinositol 3′-kinase and distinct from that induced by hypoxia. Cancer Res 2000;60:5879 – 86.

30. Stolarov J, Chang K, Reiner A, et al. Design of a retroviral-mediated ecdysone-inducible system and its application to the expression profiling of the PTEN tumor suppressor. Proc Natl Acad Sci U S A 2001;98:13043 – 8.

31. Jiang BH, Jiang G, Zheng JZ, Lu Z, Hunter T, Vogt PK. Phosphatidylinositol 3-kinase signaling controls levels of hypoxia-inducible factor 1. Cell Growth Differ 2001;12:363 – 9.

32. Fukuda R, Hirota K, Fan F, Jung YD, Ellis LM, Semenza GL. Insulin-like growth factor 1 induces hypoxia-inducible factor 1-mediated vascular endothelial cell growth factor expression, which is dependent on MAP kinase and PI-3-kinase signaling in colon cancer cells. J Biol Chem 2002; 277:38205 – 11.

33. Pore N, Gupta AK, Cerniglia GJ, Maity A. HIV protease inhibitors decrease α expression and angiogenesis in glioblastoma cells. Neoplasia 2006;8:889 – 95.

34. Liu J, Costello PC, Pham NA, et al. Integrin-linked kinase inhibitor KP-392 demonstrates clinical benefits in an orthotopic human non-small cell lung cancer model. J Thorac Oncol 2006;1:771 – 9.

35. Younes MN, Yigitbasi OG, Yazici YD, et al. Effects of the integrin-linked kinase inhibitor QLT0267 on squamous cell carcinoma of the head and neck. Arch Otolaryngol Head Neck Surg 2007;133:15 – 23.

36. Acconcia F, Manavathi B, Mascarenhas J, Talukder AH, Mills G, Kumar R. An inherent role of integrin-linked kinase-estrogen receptor α interaction in cell migration. Cancer Res 2006;66:11030 – 8.